Autotransporters but not pAA are critical for rabbit colonization by Shiga toxin-producing Escherichia coli O104:H4

Published in final edited form as:
Nat Commun. 2014 January 20; 5: 3080. doi:10.1038/ncomms4080.

Autotransporters but not pAA are critical for rabbit colonization by Shiga toxin-producing *Escherichia coli* O104:H4

Diana Munera[1,2,3], **Jennifer M Ritchie**[1,2,†], **Stavroula K Hatzios**[1,2,3], **Rod Bronson**[2], **Gang Fang**[4], **Eric E Schadt**[4], **Brigid M Davis**[1,2,3], and **Matthew K Waldor**[1,2,3,*]

[1]Division of Infectious Diseases, Brigham & Women's Hospital, Boston, MA, USA, 02115

[2]Department of Microbiology and Immunobiology, Harvard Medical School, Boston, MA, USA, 02115

[3]HHMI, Boston, MA, USA, 02115

[4]Department of Genetics and Genomic Sciences, Mount Sinai School of Medicine, New York, NY, USA, 10029

Abstract

The outbreak of diarrhea and hemolytic uremic syndrome that occurred in Germany in 2011 was caused by a Shiga toxin-producing enteroaggregative *Escherichia coli* (EAEC) strain. The strain was classified as EAEC due to the presence of a plasmid (pAA) that mediates a characteristic pattern of aggregative adherence on cultured cells, the defining feature of EAEC that has classically been associated with virulence. Here, we describe an infant rabbit-based model of intestinal colonization and diarrhea caused by the outbreak strain, which we use to decipher the factors that mediate the pathogen's virulence. Shiga toxin is the key factor required for diarrhea. Unexpectedly, we observe that pAA is dispensable for intestinal colonization and development of intestinal pathology. Instead, chromosome-encoded autotransporters are critical for robust colonization and diarrheal disease in this model. Our findings suggest that conventional wisdom linking aggregative adherence to EAEC intestinal colonization is false for at least a subset of strains.

Diarrheagenic *E. coli* is classified into six different 'pathotypes' primarily based on the patterns and mechanisms by which these pathogens adhere to cultured human cells and on presumed mechanisms of virulence (e.g., toxin production)[1]. Enteroaggregative *E. coli* (EAEC) are distinguished by their characteristic aggregative 'stacked brick' pattern of adherence to HEp-2 cells, a phenotype that is mediated by aggregative adherence plasmid (pAA)-encoded fimbriae[2]. EAEC is increasingly associated with acute and persistent

*Correspondence to: Matthew Waldor, 181 Longwood Avenue, Boston, MA, 02115. Phone: 617- 525- 4646, Fax: 617-525-4660, mwaldor@rics.bwh.harvard.edu.
†Current address: Faculty of Health and Medical Sciences, University of Surrey, Guildford, Surrey, UK, GU2 7XH.

Author Contributions

DM and MKW led the project. DM designed and performed experiments. JMR helped to develop the model; SKH helped to develop ABPP assays; RB analyzed the histopathology; GF and EES carried out the RNA-seq analysis. DM, BMD and MKW analyzed data and wrote the paper.

Competing Financial Interests

The authors have no conflicting financial interests.

Accession codes: Gene expression data have been deposited in the Sequence Read Archive database under the accession code SRS505092.

diarrheal disease in a variety of endemic settings in both the developed and developing world and in travelers[3,4]. Furthermore, EAEC has been known to cause large outbreaks of diarrhea[2]. Notably, in 2011, there was a large food-borne outbreak of diarrhea and hemolytic uremic syndrome (HUS) centered in Germany[5] caused by an atypical EAEC strain that produced Shiga toxin (Stx)[6,7]. This serogroup O104:H4 strain was classified as EAEC due to the presence of a pAA and the associated aggregative adherence on cultured cells[8]. Most EAEC strains do not produce Stx, a potent inhibitor of protein synthesis that can cause HUS and is more typically a defining feature of enterohemorrhagic *E. coli* (EHEC)[9].

Understanding of the factors and mechanisms that enable EAEC to colonize the intestine and cause diarrhea has been hampered by the marked genetic heterogeneity of EAEC strains, both at chromosomal and pAA-encoded loci[1,2]. A variety of putative virulence factors, including plasmid- and chromosome-encoded toxins and fimbriae, have been described, but to date no single or set of putative virulence-associated gene(s) is found in all EAEC[1]. Studies of EAEC pathogenicity have also been hindered by a lack of suitable animal models for testing the importance of putative colonization and virulence factors[1]. Some initial studies were plagued by a lack of reliable intestinal colonization[10–12], perhaps due to the presence of normal intestinal flora. Although treatment of animals with antibiotics can prevent this difficulty, colonized animals often do not exhibit intestinal manifestations of disease, such as diarrhea and inflammation, either in response to classical (Stx-) EAEC or to the outbreak-linked Stx2+ isolates[12–14]. For example, although outbreak-linked O104:H4 isolates induce kidney damage in ampicillin-treated mice[14], it does not cause pathological changes in the murine intestine. Additionally, studies with antibiotic-treated animals have not reliably confirmed the importance of factors known to be important for pathogenesis in humans, such as the Type 3 secretion system that is critical for the virulence of EHEC[15,16]. In contrast, our previous studies using infant rabbit models of EHEC, *Vibrio cholerae*, and *V. parahaemolyticus* infection have revealed close similarities between factors required in humans and infant rabbits for intestinal colonization, induction of diarrhea, and histopathological signs of disease, suggesting that rabbits are excellent model hosts for investigation of enteric pathogens[17–20].

Here, we report the development of an infant rabbit-based animal model of intestinal disease caused by Stx-producing *E. coli* O104:H4, which we use to decipher the factors that enable this pathogen to colonize the intestine and cause disease. As anticipated, our studies confirm the causal role of Stx in diarrhea. Additionally, they suggest that putative adherence fimbriae and other pAA-encoded factors are not required for intestinal colonization by EAEC, and that chromosome-encoded autotransporters are more significant for robust colonization and subsequent induction of diarrheal disease.

Results

Stx$^+$ EAEC induces intestinal disease in infant rabbits

To investigate the pathogenicity of *E. coli* O104:H4, 2-day-old rabbits were orogastrically inoculated with a clinical isolate from the 2011 German outbreak, C227-11 (here referred to as C227), whose genome had been sequenced[6]. Nearly all rabbits inoculated with C227 developed diarrhea and/or intestinal fluid accumulation by 3 days post-inoculation (PI), while mock-infected rabbits did not display any signs of disease (Table 1). The majority of C227 colony forming units (cfu) were detected in homogenates of the cecum and colon of infected animals, although bacteria were also recovered from the distal small intestine (Fig. 1). Peak colonization occurred 2–3 days PI and diminished thereafter (Fig. 2). Immunofluoresence microscopy revealed that C227 cells were primarily present as large aggregates in the intestinal lumen, and were often apparently attached to luminal contents (Fig. 3a and Supplementary Fig. 1). Individual C227 cells were also attached to the

epithelial surface, but did not markedly disrupt the underlying epithelium. Statistically significant increases in inflammation (marked by infiltration of heterophils (rabbit equivalent of neutrophils)) and apoptosis of epithelial cells were evident in the colonic and cecal epithelia but not in the small intestines of infected rabbits (Fig. 3b, c and Supplementary Fig. 2). Breaching of the colonic epithelial permeability barrier, measured as increased uptake of biotin relative to mock-infected animals, was also observed (Fig. 3d), but renal pathology was not detected. Our data suggests that diarrhea in response to C227 infection is not linked to marked disruption of the intestinal epithelium, as seen with some pathogens[20], but instead is associated with inflammation and more subtle alterations in epithelial barrier function.

Stx is essential for C227-induced diarrhea and histopathology

C227, like other isolates from the 2011 German outbreak, encodes numerous putative virulence factors, including the prophage-borne *stx*$_2$*AB*, which encode the A and B subunits of Shiga toxin 2 (Stx2). This toxin, a potent inhibitor of protein synthesis, is a critical virulence factor in EHEC both in infected humans and in our infant rabbit model of EHEC infection[9,17]. C227 and EHEC O157:H7 produce similar amounts of Stx2 *in vitro* (Supplementary Fig. 3). Notably, a C227 mutant lacking *stx*$_2$*AB* (Δ*stx2*) colonized the rabbit intestine in a similar fashion as the wild type strain; however, animals inoculated with this mutant did not exhibit diarrhea or impairment of the colonic epithelial permeability barrier, and they showed a marked reduction in heterophil infiltration and apoptosis in the colonic and cecal epithelium relative to C227-infected animals (Table 1, Fig. 1, and Fig. 3c, d). Collectively, these observations are consistent with previous observations linking Stx2 to diarrhea and inflammation in rabbits infected with EHEC[17] and to apoptosis in toxin treated animals[21]. They also suggest that Stx2 disrupts the intestinal permeability barrier in C227 infected animals, potentially either directly, by intoxicating epithelial cells, or indirectly, through induction of inflammation and apoptosis. The critical role of Stx2 in rabbit pathogenesis supports the prevailing analysis during the German outbreak that the presence of a prophage encoding *stx*$_2$*AB* rendered outbreak-linked strains far more pathogenic than typical EAEC isolates[6,22]. This finding is also compatible with results from a study of antibiotic-treated mice infected with *E. coli* O104:H4 +/− a toxin-encoding prophage[14]; however, our study more conclusively links virulence to the presence of Stx2, as it rules out possible effects of other phage-encoded factors, such as a restriction/modification system previously shown to modulate expression of numerous bacterial loci[23].

pAA is dispensable for colonization by O104:H4 strains

Though highly heterogeneous in gene content, EAEC strains harbor a plasmid (pAA) that mediates aggregative adherence to tissue-cultured cells (via plasmid-encoded Aggregative Adherence Fimbria) and encodes several additional putative virulence factors[24]. We isolated a C227 derivative that had spontaneously lost its pAA, which as expected no longer exhibited aggregative adherence to cultured HEp-2 cells (Fig. 4a). Surprisingly, the overall accumulation and intestinal distribution of the plasmid-free strain in rabbit intestines were equivalent to those of the wild type strain (Fig. 1 and Supplementary Fig. 4), and the two strains induced equivalent frequency/intensity of diarrhea, inflammation and apoptosis (Table 1 and Fig. 3c). Additionally, comparative analyses of C227 gene expression under laboratory conditions (in LB medium) and during infection (assessed using RNA isolated from organisms within the cecal fluid of infected rabbits) revealed that of the 51 pAA genes that were differentially expressed between these two conditions, 42 (82%) showed reduced expression *in vivo* (Fig. 4b). These 42 genes included several putative virulence genes, e.g., the putative virulence regulator *aggR*, *aggACD* (encodes AAF-I), *aap* (dispersin), and *aatPABCD* (the dispersin translocator) (Fig. 4b, Supplementary Table S1). Thus, our analyses all suggest that despite their impact on bacterial adhesion *in vitro*, pAA-encoded

adhesins and other gene products are not required for intestinal colonization or subsequent development of C227-based intestinal pathology in this animal model of disease.

To investigate whether pAA plays a more significant role in intestinal colonization by other O104:H4 strains, we isolated a derivative of 55989 (a non-Shiga toxin-producing EAEC O104:H4 strain[25]) that lacked its AA plasmid. As anticipated, loss of pAA eliminated 55989's aggregative adherence to Hep-2 cells (Fig. 4a). However, there was no difference between intestinal colonization by 55989 harboring or lacking pAA (Fig. 4c). Thus, our experiments suggest that at least for serogroup O104:H4 strains, AA plasmids do not play a significant role in intestinal adhesion or colonization. Our results are consistent with a very recent analysis of bacterial isolates from the German outbreak and a recent study using ampicillin-treated mice, in which loss of pAA during the progression of an infection was frequently detected[14,26], and provide the first indication that establishment (rather than maintenance) of an intestinal infection is not necessarily dependent on pAA. However, we should note that analyses of human isolates did suggest that the presence of pAA augments the likelihood of HUS associated with $Stx2^+$ EAEC infection. This hypothesis cannot be evaluated using our animal model, since infant rabbits do not develop HUS or other renal pathology, either in response to EHEC infection or to $Stx2^+$ EAEC. Thus, while our data suggest that pAA does not contribute to establishment of intestinal infections by C227 or other O104:H4 EAEC, which is a prerequisite for induction of diarrhea and intestinal pathology, we cannot fully rule out a role for the plasmid in subsequent stages of *E. coli* O104:H4-induced disease, or exclude the possibility that distinct factors mediate disease in humans and infected animals. Whether AA plasmids promote colonization by other diverse EAEC serogroups remains an open question.

SPATEs promote C227 intestinal colonization and disease

Although the presence of pAA is the defining feature of EAEC, and pAA has been presumed to contribute to EAEC virulence, human volunteer studies have demonstrated that the presence of pAA is not sufficient for pathogenicity[27]. Other factors hypothesized to play a role in pathogenesis are the Serine Protease Autotransporters of Enterobacteriaceae (SPATEs), which are produced by a variety of pathogenic *E. coli*, *Shigella* and *Salmonella*[28,29]. These autotransporter proteins are comprised of an N-terminal signal peptide for targeting the protein to the periplasm, followed by a secreted 'passenger' domain (containing the serine protease) and a β domain that promotes the translocation and targeting of the passenger domain to the outer membrane in a multistep process catalyzed by the Bam complex[30,31]. The N terminus is subsequently released from the cell via SPATE autocleavage[29] (Fig. 5a, b), and typically is among its producer's most abundant secreted proteins. Almost all (95%) EAEC isolates encode at least one SPATE, while a far lower percentage of other *E. coli* pathotypes produce these proteins[32]. The Shiga toxin-producing EAEC O104:H4 strain that caused the German outbreak contains genes encoding 3 different SPATES. Two of these, *sigA*[33,34] and *pic*[12,35], which is encoded in two identical copies, are located on chromosomal pathogenicity islands, while the third, *sepA*[36], is found on pAA. All three SPATEs were detected in supernatants from C227 cultures as active serine proteases using an activity-based probe (Fig. 5c). SepA is clearly not required for C227 pathogenicity, since colonization and virulence of C227 and C227ΔpAA were indistinguishable. In contrast, deletion of either *sigA* or both copies of *pic* (which was confirmed using the activity-based assay of secreted proteins; Fig. 5c) reduced intestinal colonization 3 days PI by ~3 orders of magnitude (Fig. 1). The attenuation in the colonization of the SPATE mutants was less dramatic 2 days PI (Supplementary Fig. 4), suggesting that these autotransporters may promote the persistence of the pathogen in the gastrointestinal tract. As expected, the absence of these SPATEs did not alter aggregative adherence of C227 (Supplementary Fig. 5).

SigA release but not protease activity mediates colonization

Analysis of a wt revertant derived from C227Δ*sigA* (SigA^{wt}) confirmed that the attenuation of C227Δ*sigA* results from absence of SigA: C227 SigA^{wt} caused diarrhea and colonized rabbit intestines in a similar fashion as wild type C227 (Fig. 5d, Table 2, and Fig. 6). Unexpectedly, a *sigA* point mutant that lacks serine protease activity (SigA^{sp}; SigA S258A; Fig. 5d) also displayed virulence equivalent to that of the wt strain (Table 2 and Fig. 6), suggesting that SigA substrate cleavage does not contribute to C227 pathogenesis. However, a *sigA* point mutant that lacks an autocleavage site and hence is not released from the cell surface into supernatants (SigA^{cl}; SigA N1008A, N1009A; Fig. 5d) was as highly attenuated in infant rabbits as C227Δ*sigA* (Table 2 and Fig. 6). Secreted colonization factors are rare, but have been described in other bacterial pathogens[37]. SigA's precise role remains to be defined; analysis of the effects of SigA, Pic, and additional SPATEs on the virulence of diverse EAEC isolates are also warranted, in order to clarify whether this family of proteins routinely contributes to pathogenesis.

Discussion

Classification of diarrheagenic *E. coli* based on patterns of adherence to tissue-cultured cells[1,38] has been a useful heuristic, as in many cases *in vitro*-based classifications reflect consistent pathology *in vivo*. However, our findings in the infant rabbit model that pAA-based aggregative behavior is not linked with intestinal colonization by strains classified as EAEC, coupled with the known genetic heterogeneity of EAEC isolates, suggests that at least for this subset of pathogenic *E. coli*, shared adherence phenotypes may have masked recognition of important colonization and virulence mechanisms. Our data further suggest that strain-specific factors and mechanisms, such as autotransporters, may play a more prominent role in pathogenicity than previously recognized. Our new infant rabbit model of EAEC infection should be extremely useful for preliminary identification and analyses of such factors.

Methods

Ethics statement

The animal protocols used for the studies described here were reviewed and approved by the Harvard Medical Area Standing Committee on Animals (IACUC protocol #04308, Animal Welfare Assurance of Compliance #A3431-01). All animal studies were carried out in accordance with the recommendations in the Guide for the Care and Use of Laboratory Animals of the National Institutes of Health (8th Edition) and the Animal Welfare Act of the United States Department of Agriculture.

Bacterial strains and plasmids and growth conditions

Strains, plasmids, and primers used in this study are listed in Supplementary Tables S2, S3 and S4 respectively. The *E. coli* O104:H4 German outbreak strain isolate C227-11 (C227)[6] and EAEC O104:H4 strain 55989 (55989)[25] were the wild type strains used in this study. Isogenic mutants of C227 were constructed by standard allele exchange techniques[39] using derivatives of suicide vectors pDS132 or pDM4 harboring DNA regions flanking *stx*$_2$*AB*, *sigA* and *pic* (Supplementary Tables S3 and S4); the two identical *pic* copies were deleted in a sequential fashion. C227Δ*sigA* was used as the starting strain to generate *sigA*^{wt}, *sigA*^{sp}, *sigA*^{cl} and *sigA*^{sp,cl} mutants with allele replacement vectors pDM4-flk-sigA(wt), pDM4-flk-sigA(S258A), pDM4-flk-sigA(N1008A, N1009A) and pDM4-flk-sigA(S258A, N1008A, N1009A) respectively. *E. coli* strain MFD*pir* was used as donor strain to deliver allele exchange vectors by conjugation to recipient EAEC strains. PCR and sequencing was used to confirm all the mutants used in this study. Serial passages in culture were used to isolate

C227 and 55989 mutants that lost their respective pAA plasmids, which was established by PCR tests of internal fragments for plasmid loci *aggR*, *aatA*, *aatB*, *sepA*, *aap* and chromosomal encoded *lacZ* as positive control (Supplementary Fig. 6 and Supplementary Table 4). All strains were routinely grown in LB medium or on LB agar plates containing the appropriate antibiotics at the following concentrations: 20 μg/mL chloramphenicol and 200 μg/mL streptomycin. Growth curves of wild type strains and their derivatives (Supplementary Fig. 7) did not reveal detectable differences in the generation times of the strains used in this work.

Infant rabbit infection studies

Litters of 2-day-old New Zealand White infant rabbits (both genders) with the lactating doe were acquired from a commercial breeder. The same day, the rabbits were administered ranitidine intraperitoneally (2 μg/g) and 3 hr later they were orogastrically inoculated with 1 x 10^9 cfu of the EAEC strain (suspended in sodium bicarbonate solution (pH 9)) using a size 4 French catheter.

Following inoculation, the infant rabbits were monitored at least 2x/day for signs of illness. At euthanasia, disease was scored as follows: no gross disease (no adherent fecal material on fur and intestines appear normal), intestinal fluid (no adherent fecal material on fur but intestines swollen with fluid), diarrhea (liquid fecal material stains adherent to fur, and intestines swollen with fluid). The number of C227 or 55989 cfu in tissue samples taken from ileum, cecum, proximal colon, mid colon, distal colon and stools was determined after homogenization, serial dilution and plating on LB media containing 200 μg mL^{-1} streptomycin[19]. For sections where no colonies were detected at the lowest dilution plated, the cfu were calculated using the lower limit of detection as a value.

Histopathology and immunofluorescence microscopy

For histological analyses, tissue sections were fixed in 10% neutral buffered formalin, processed for paraffin embedding and stained with hematoxylin and eosin (H&E). Slides were examined using a Zeiss AxioImager M1 microscope at 40x magnification with an AxioCamMR Camera and processed using Axio Vision 4.8 LE software (Zeiss). The slides were semi-quantitatively assessed for apoptosis and infiltration of heterophils by a pathologist blinded to the origin of the tissue. Each histological parameter was evaluated on a 0–3 scale as follows: 0 (normal), 1 (mild), 2 (moderate) and 3 (severe). Tissue sections used for immunofluorescence studies were fixed in 4% paraformaldehyde (in PBS) on ice for 2 h before being placed in 30% sucrose (in PBS) at 4°C overnight. The next day, the tissue segments were briefly washed in PBS, the outer surface was dried on filter paper, and trimmed pieces were placed in optimal cutting temperature (OCT) compound (Electron Microscopy Sciences, PA). Each tissue block was quick-frozen over a mixture of dry ice and ethanol and stored at −80°C prior to sectioning. Sections that were approximately 5-μm thick were cut, placed on glass slides, and processed for immunofluorescence. Initially, OCT compound was removed from the tissue section by washing the slides three times in PBS (5 min each). For detection of C227, chicken polyclonal antisera generated against heat-killed C227 (Lampire) was employed in combination with an anti-IgY chicken-FITC conjugate (Abcam). Slides were examined for fluorescence using a Zeiss LSM510 Meta upright confocal microscope at 63x magnification.

Biotin permeability

Biotin was used as a tracer molecule to determine the integrity of the epithelial barrier[20]. Briefly, immediately after removal of the entire intestinal tract from mock, C227 or Δ*stx2* infected rabbits, the colonic tissue was separated while maintaining their correct orientation (ie proximal vs distal ends). EZ-Link Sulfo-NHS-Biotin (Thermo Scientific, IL) was

injected slowly (1–2 min) into the lumen via the open (cut) end of the most distal part of the colon. After 3 min, the tissue section just proximal to the site of injection was removed, fixed in 4% paraformaldehyde and processed for immunofluorescence staining as described above. Tissue sections were incubated with streptavidin linked to Alexa 546 (1/500) (S11225; Invitrogen) for 1 hr at room temperature before being counterstained with phalloidin Alexa fluor 633 and DAPI. Colonic tissue from mock, C227 or Δ*stx2* infected rabbits that were not treated with biotin exhibited no background staining following incubation with streptavidin only.

Hep-2 cell-adherence assay

HEp-2 cell-adherence assays were carried out as described previously[40] with the following modifications. HEp-2 cells (ATCC CCL-23) were grown for 24 h to 50–60 % confluence on 13 mm diameter coverslips in 24-well tissue-culture plates in Minimum Essential Medium (MEM) supplemented with 10 % fetal calf serum (FBS; Sigma) at 37°C in a 5% CO_2 atmosphere. On the day of the assay the HEp-2 cells were washed with MEM containing 1% D-mannose (Sigma-Aldrich) in PBS and 1 ml of this media was added to each well. Infections were performed in triplicates with 25 μl/well of the indicated strain grown at 37°C static for 16–18 hours. After 3 hours of incubation at 37°C in a 5% CO_2 atmosphere, unbound bacteria were removed by washing three times with DPBS (Sigma). Cells were fixed with 3% paraformaldehyde for 20 min at RT before washing in PBS. For immunostaining, the fixed cells were quenched for 20 min with PBS/ 50 mM NH_4Cl, permeabilized for 4 min in PBS/ 0.1% Triton X-100 and washed 3 times in PBS. The coverslips were then blocked for 10 min with 1% BSA in PBS, incubated with C227 chicken polyclonal antisera (1/200) 1 h at RT, washed in PBS, blocked, and incubated with goat anti-chicken FITC secondary antibody (1/200), Alexa Fluor Phalloidin 568 (1/100) and DAPI (1 $\mu g\ mL^{-1}$) 1 h at RT in the dark. After washing 3 times with PBS and 3 times with MiliQ water, coverslips were mounted on slides using ProLong Gold anti-fade reagent (Invitrogen).

RNA sequencing and analysis

RNA was isolated from triplicate mid-exponential phase (O.D.≈0.6) C227 cultures grown in LB at 37°C and from the cecal fluid of two C227-infected rabbits[41]. RNA samples were treated with RiboZero bacterial Gram Negative ribosomal removal kit (Epicentre; MRZGN126). For cDNA library preparation[23,41], rRNA-depleted RNA was chemically fragmented and then reverse transcribed with SuperScript III (Invitrogen) using random hexamers. The cDNA was converted to dsDNA, end repaired, 5′ adenylated and then ligated to DNA adapters enabling Illumina sequencing using the NEB Next mRNA-seq kit (New England BioLabs; E6100S). PCR for 16 cycles using KAPA HiFi HotStart DNA Polymerase was performed to incorporate Illumina specific sequences and molecular barcodes. The Illumina HiSeq 2000 with a read length of 100 nt was used for sequencing. Reads were mapped to the TY-2482 reference genome. A gene was included for differential expression analysis if it had more than one count per million reads (CPM≥1) in at least two samples. For the differential expression results depicted in Fig. 4b, the program edgeR was used to detect significantly differentially expressed genes at a false discovery rate < 0.01. To display the expression data in Fig. 4b, expression values were converted into a Z score by subtracting the mean expression value and dividing by the standard deviation for each gene over all samples scored. Gene expression data have been deposited in the Sequence Read Archive database (www.ncbi.nlm.nih.gov/Traces/sra/) under accession number SRS505092.

Activity-Based Protein Profiling (ABPP) assays

To test the serine protease activity of SPATEs, 5 ml cultures were grown at 37°C with shaking for 24 hours. Filtered concentrated culture supernatants were quantified and normalized to the total protein. To analyze SPATE activity in whole cells, 200 μl of each culture was pelleted, washed with PBS and resuspended in PBS. Duplicates of 44 μl of each supernatant and whole cells sample were prepared and PMSF (25 mM final concentration) was added to one sample to specifically inactivate serine proteases while the same amount of ethanol was added to other sample. After incubation at 37°C for 30 min, all samples were reacted with 2mM of ActivX TAMRA-FP (Thermo Scientific), a serine hydrolase probe, for 1 h at RT in the dark. Samples were prepared under denaturing (1% SDS, 95°C, 5 min) conditions and 15 μl of each sample were separated on SDS-PAGE 3–8% Tris-acetate gels, using standard methods[42]. Gels were fluorescence-scanned using a FLA-5100 Imager Reader (Fujifilm). The protein content in the samples was visualized after separation on SDS-PAGE 3–8% Tris-acetate gels with coomassie[42]. Full fluorescence-scanned blots and coomassie-stained gels are shown in Supplementary Fig. 8.

Supplementary Material

Refer to Web version on PubMed Central for supplementary material.

Acknowledgments

We are grateful to members of the Waldor lab for helpful comments on this manuscript and to the Harvard Digestive Disease Center Imaging Core for assistance with confocal microscopy. This work was supported by grants from HHMI and NIH R37 AI-42347 (MKW).

References

1. Croxen M, Finlay B. Molecular mechanisms of *Escherichia coli* pathogenicity. Nat Rev Microbiol. 2010; 8:26–38. [PubMed: 19966814]
2. Harrington S, Dudley E, Nataro J. Pathogenesis of enteroaggregative *Escherichia coli* infection. FEMS Microbiol Lett. 2006; 254:12–18. [PubMed: 16451173]
3. Bhan M, et al. Enteroaggregative *Escherichia coli* associated with persistent diarrhea in a cohort of rural children in India. J Infect Dis. 1989; 159:1061–1064. [PubMed: 2656875]
4. Cravioto A, et al. Association of *Escherichia coli* HEp-2 adherence patterns with type and duration of diarrhoea. Lancet. 1991; 337:262–264. [PubMed: 1671111]
5. Frank C, et al. Epidemic profile of Shiga-toxin-producing *Escherichia coli* O104:H4 outbreak in Germany. N Engl J Med. 2011; 365:1771–1780. [PubMed: 21696328]
6. Rasko D, et al. Origins of the *E. coli* strain causing an outbreak of hemolytic-uremic syndrome in Germany. N Engl J Med. 2011; 365:709–717. [PubMed: 21793740]
7. Rohde H, et al. Open-source genomic analysis of Shiga-toxin-producing *E. coli* O104:H4. N Engl J Med. 2011; 365:718–724. [PubMed: 21793736]
8. Bielaszewska M, et al. Characterisation of the *Escherichia coli* strain associated with an outbreak of haemolytic uraemic syndrome in Germany, 2011: a microbiological study. Lancet Infect Dis. 2011; 11:671–676. [PubMed: 21703928]
9. Johannes L, Romer W. Shiga toxins--from cell biology to biomedical applications. Nat Rev Microbiol. 2010; 8:105–116. [PubMed: 20023663]
10. Kang G, Pulimood A, Mathan M, Mathan V. Enteroaggregative *Escherichia coli* infection in a rabbit model. Pathology. 2001; 33:341–346. [PubMed: 11523937]
11. Sainz T, et al. Histological alterations and immune response induced by Pet toxin during colonization with enteroaggregative *Escherichia coli* (EAEC) in a mouse model infection. J Microbiol. 2002; 40:91–97.

12. Harrington S, et al. The Pic protease of enteroaggregative *Escherichia coli* promotes intestinal colonization and growth in the presence of mucin. Infect Immun. 2009; 77:2465–2473. [PubMed: 19349428]
13. Torres A, et al. *In vivo* bioluminescence imaging of *Escherichia coli* O104:H4 and role of aerobactin during colonization of a mouse model of infection. BMC Microbiol. 2012; 12:112. [PubMed: 22716772]
14. Zangari T, et al. Virulence of the Shiga toxin type 2-expressing *Escherichia coli* O104:H4 German outbreak isolate in two animal models. Infect Immun. 2013; 81:1562–1574. [PubMed: 23439303]
15. Wadolkowski E, Burris J, O'Brien A. Mouse model for colonization and disease caused by enterohemorrhagic *Escherichia coli* O157:H7. Infect Immun. 1990; 58:2438–2445. [PubMed: 2196227]
16. Wadolkowski E, Sung L, Burris J, Samuel J, O'Brien A. Acute renal tubular necrosis and death of mice orally infected with *Escherichia coli* strains that produce Shiga-like toxin type II. Infect Immun. 1990; 58:3959–3965. [PubMed: 2254023]
17. Ritchie J, Thorpe C, Rogers A, Waldor M. Critical roles for *stx2*, *eae*, and *tir* in enterohemorrhagic *Escherichia coli*-induced diarrhea and intestinal inflammation in infant rabbits. Infect Immun. 2003; 71:7129–7139. [PubMed: 14638803]
18. Ritchie J, Waldor M. The locus of enterocyte effacement-encoded effector proteins all promote enterohemorrhagic *Escherichia coli* pathogenicity in infant rabbits. Infect Immun. 2005; 73:1466–1474. [PubMed: 15731044]
19. Ritchie J, Rui H, Bronson R, Waldor M. Back to the future: Studying Cholera pathogenesis using infant rabbits. mBio. 2010; 1:e00047–10. [PubMed: 20689747]
20. Ritchie J, et al. Inflammation and disintegration of intestinal villi in an experimental model for *Vibrio parahaemolyticus*-induced diarrhea. PLoS Pathog. 2012; 8:e1002593. [PubMed: 22438811]
21. Tesh V. The induction of apoptosis by Shiga toxins and ricin. Curr Top Microbiol Immunol. 2012; 357:137–178. [PubMed: 22130961]
22. Karch H, et al. The enemy within us: lessons from the 2011 European *Escherichia coli* O104:H4 outbreak. EMBO Mol Med. 2012; 4:841–848. [PubMed: 22927122]
23. Fang G, et al. Genome-wide mapping of methylated adenine residues in pathogenic *Escherichia coli* using single-molecule real-time sequencing. Nature Biotechnol. 2012; 30:1232–1239. [PubMed: 23138224]
24. Johnson T, Nolan L. Pathogenomics of the virulence plasmids of *Escherichia coli*. Microbiol Mol Biol Rev. 2009; 73:750–774. [PubMed: 19946140]
25. Bernier C, Gounon P, Le Bouguénec C. Identification of an Aggregative Adhesion Fimbria (AAF) Type III-Encoding Operon in Enteroaggregative *Escherichia coli* as a Sensitive Probe for Detecting the AAF-Encoding Operon Family. Infect Immun. 2002; 70:4302–4311. [PubMed: 12117939]
26. Zhang W, et al. Lability of the pAA Virulence Plasmid in *Escherichia coli* O104:H4: Implications for Virulence in Humans. PloS one. 2013; 8:e66717. [PubMed: 23805269]
27. Nataro JP, et al. Heterogeneity of enteroaggregative *Escherichia coli* virulence demonstrated in volunteers. J Infect Dis. 1995; 171:465–468. [PubMed: 7844392]
28. Dautin N. Serine protease autotransporters of enterobacteriaceae (SPATEs): biogenesis and function. Toxins. 2010; 2:1179–1206. [PubMed: 22069633]
29. Ruiz-Perez F, Nataro J. Bacterial serine proteases secreted by the autotransporter pathway: classification, specificity, and role in virulence. Cell Mol Life Sci. 201310.1007/s00018-013-1355-8
30. Pavlova O, Peterson J, Ieva R, Bernstein H. Mechanistic link between β barrel assembly and the initiation of autotransporter secretion. Proc Natl Acad Sci USA. 2013; 110:47.
31. Grijpstra J, Arenas J, Rutten L, Tommassen J. Autotransporter secretion: varying on a theme. Res Microbiol. 2013; 164:562–582. [PubMed: 23567321]
32. Boisen N, Ruiz-Perez F, Scheutz F, Krogfelt KA, Nataro JP. Short report: high prevalence of serine protease autotransporter cytotoxins among strains of enteroaggregative *Escherichia coli*. Am J Trop Med Hyg. 2009; 80:294–301. [PubMed: 19190229]

33. Al-Hasani K, et al. The *sigA* gene which is borne on the she pathogenicity island of *Shigella flexneri 2a* encodes an exported cytopathic protease involved in intestinal fluid accumulation. Infect Immun. 2000; 68:2457–2463. [PubMed: 10768931]
34. Al-Hasani K, Navarro-Garcia F, Huerta J, Sakellaris H, Adler B. The immunogenic SigA enterotoxin of *Shigella flexneri 2a* binds to HEp-2 cells and induces fodrin redistribution in intoxicated epithelial cells. PloS one. 2009; 4:e8223. [PubMed: 20011051]
35. Navarro-Garcia F, et al. Pic, an autotransporter protein secreted by different pathogens in the Enterobacteriaceae family, is a potent mucus secretagogue. Infect Immun. 2010; 78:4101–4109. [PubMed: 20696826]
36. Benjelloun-Touimi Z, Sansonetti P, Parsot C. SepA, the major extracellular protein of *Shigella flexneri*: autonomous secretion and involvement in tissue invasion. Mol Microbiol. 1995; 17:123–135. [PubMed: 7476198]
37. Kirn T, Bose N, Taylor R. Secretion of a soluble colonization factor by the TCP type 4 pilus biogenesis pathway in *Vibrio cholerae*. Mol Microbiol. 2003; 49:81–92. [PubMed: 12823812]
38. Kaper J, Nataro J, Mobley H. Pathogenic *Escherichia coli*. Nat Rev Microbiol. 2004; 2:123–140. [PubMed: 15040260]
39. Donnenberg M, Kaper J. Construction of an *eae* deletion mutant of enteropathogenic *Escherichia coli* by using a positive-selection suicide vector. Infect Immun. 1991; 59:4310–4317. [PubMed: 1937792]
40. Jenkins C, et al. Detection of enteroaggregative *Escherichia coli* in faecal samples from patients in the community with diarrhoea. J Med Microbiol. 2006; 55:1493–1497. [PubMed: 17030907]
41. Mandlik A, et al. RNA-Seq-based monitoring of infection-linked changes in *Vibrio cholerae* gene expression. Cell Host Microbe. 2011; 10:165–174. [PubMed: 21843873]
42. Sambrook, J.; Fritsch, EF.; Maniatis, T. Molecular cloning: a laboratory manual. 2. New York: 1989.

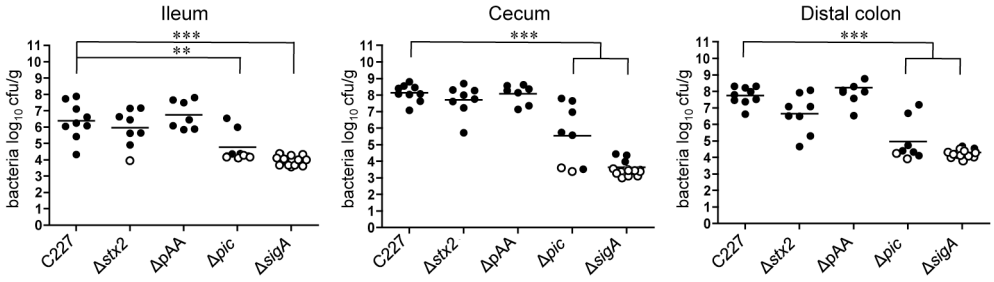

Figure 1. Intestinal colonization in infant rabbits inoculated with *E. coli* C227 or isogenic mutants

Concentration (cfu g^{-1}) of bacteria recovered 3 days PI from homogenates of intestinal tissues from rabbits infected with the indicated strain. Data points represent individual rabbits (C227, n=9; Δ*stx2*, n=8; ΔpAA, n=7; Δ*pic*, n=8; Δ*sigA*, n=13). Open symbols represent the limit of detection for samples from which no cfu were isolated. Bars show the geometric mean. Statistical analysis was performed using one way ANOVA and Bonferroni's multiple comparison post-test; ** $P < 0.01$ and *** $P < 0.001$.

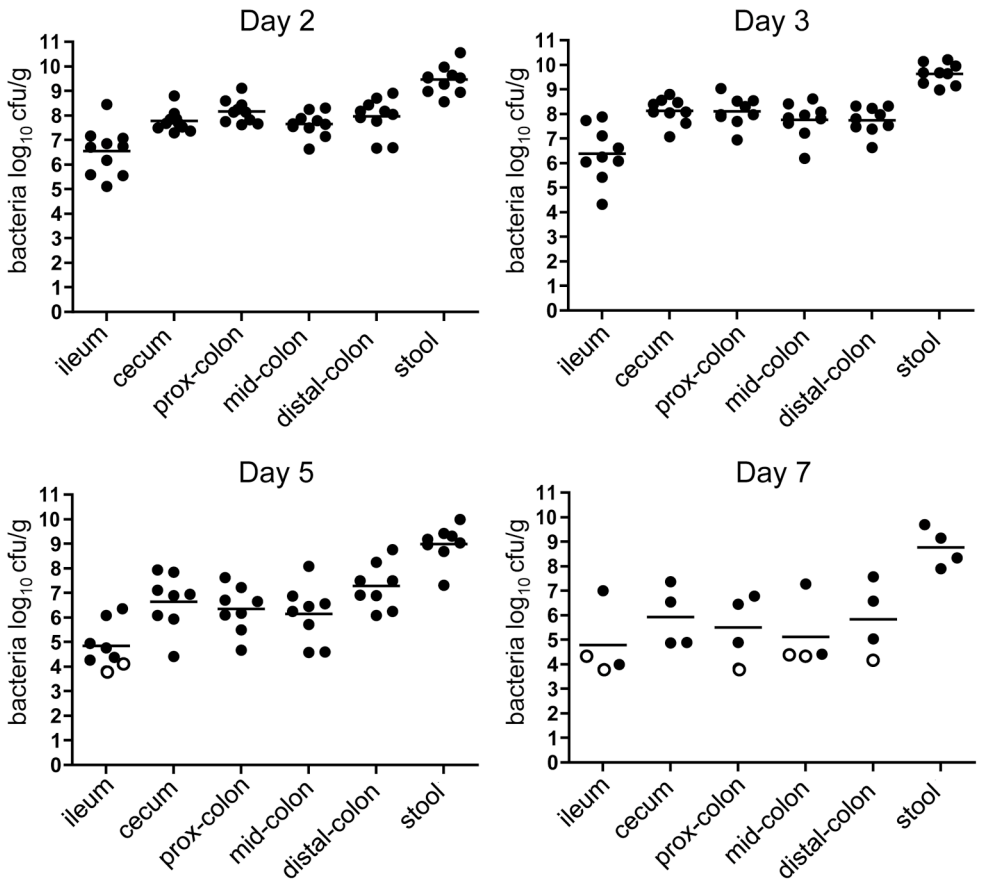

Figure 2. Kinetics of C227 colonization in infant rabbits

Concentration (cfu g^{-1}) of bacteria recovered from homogenates of intestinal tissues or stools from rabbits infected with wild type C227 at different times after infection. Data points represent individual rabbits (day 2, n=10; day 3, n=9; day 5, n=8; day 7, n=4). Open symbols represent the limit of detection for samples from which no cfu were isolated. Bars show the geometric mean.

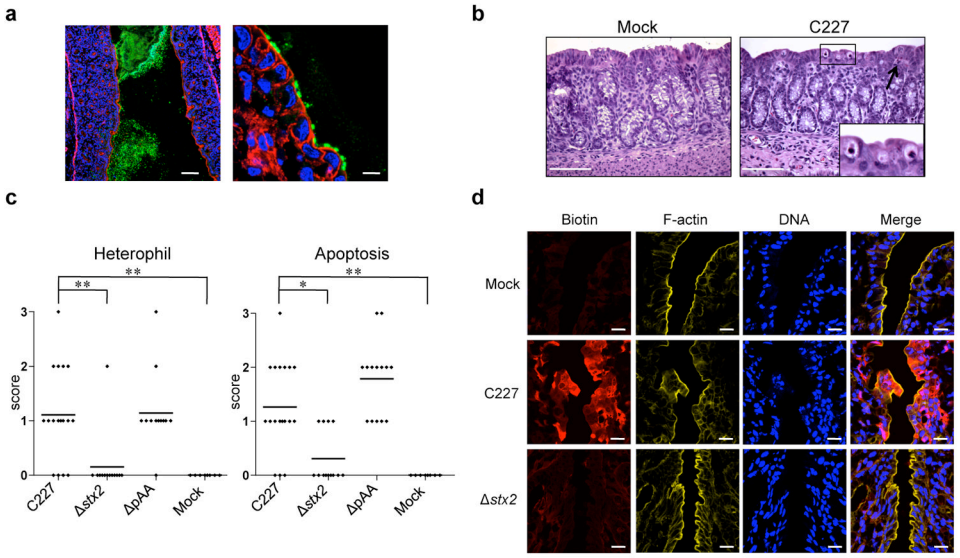

Figure 3. Histopathology in infant rabbits inoculated with *E. coli* C227 or isogenic mutants

(**a**) Representative confocal micrographs showing C227 in the intestinal lumen and attached to intestinal tissue at day 3 PI in the distal colon. C227 was stained with polyclonal antisera against C227 (green) and counterstained with phalloidin-Alexa 568 (red) and DAPI (blue) to detect F-actin and nuclei, respectively. Scale bar = 100 μm (left panel) and 10 μm (right panel). (**b**) Representative H&E-stained colonic sections from C227 and mock-infected rabbits 3 days PI showing infiltration of heterophils (arrow) and apoptosis (enlarged box). Scale bar=100 μm. (**c**) Pathology scores for infiltration of heterophils and apoptosis in the distal colon of rabbits inoculated with the indicated strain. Data points represent individual rabbits from 2 and 3 days PI (C227, n=19; Δ*stx2*, n=13; ΔpAA, n=14; Mock, n=8). Statistical analysis was performed using Kruskal-Wallis statistic with Dunn's post-test for multiple comparisons. * $P < 0.05$, ** $P < 0.01$. (**d**) Colonic tissue from rabbits infected with the indicated strain stained with biotin (red) prior to sectioning, then counterstained with DAPI (blue) and phalloidin-Alexa 633 (yellow). Scale bar=20 μm.

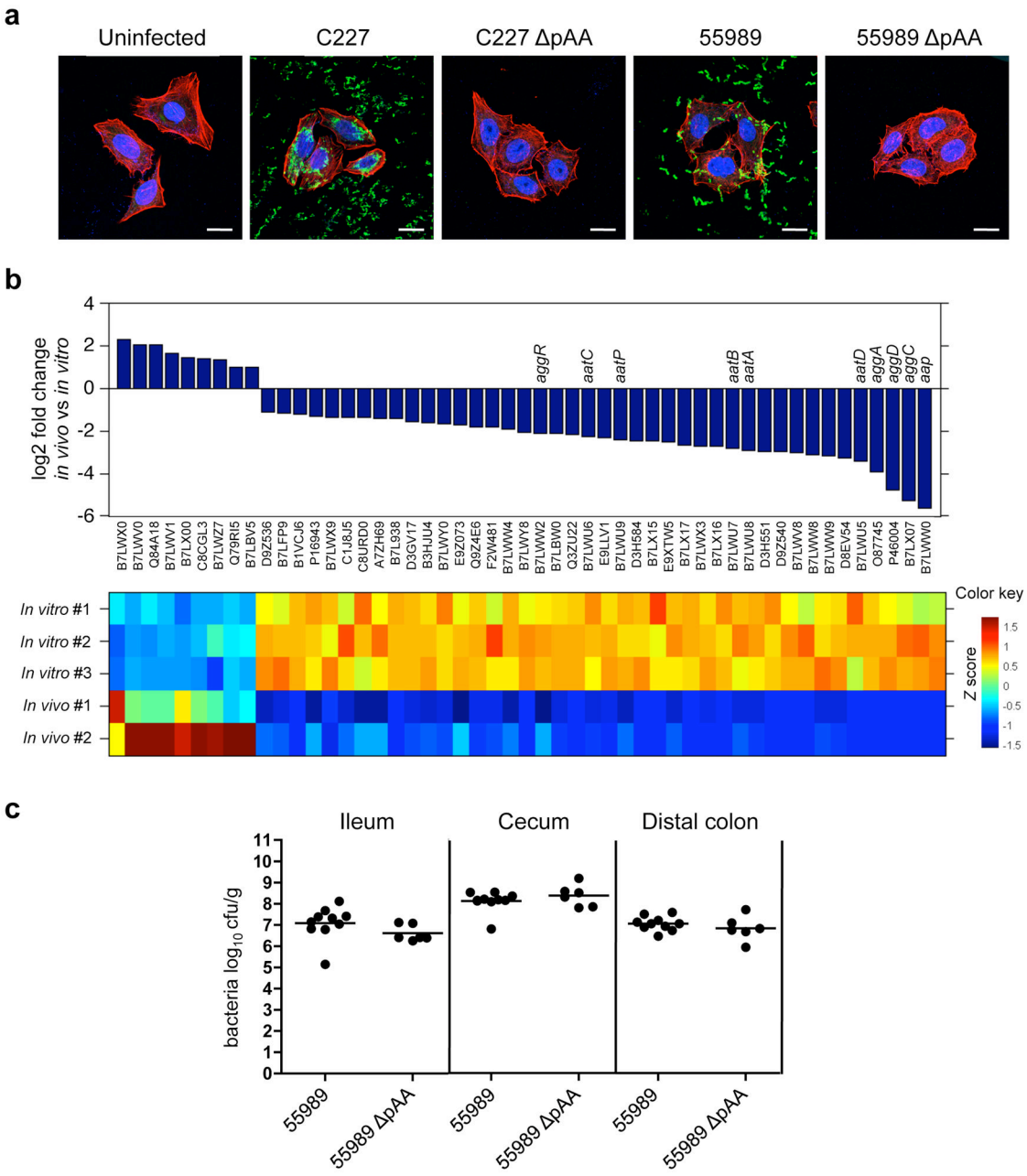

Figure 4. The role of pAA in virulence of O104:H4 EAEC

(**a**) Adherence of EAEC to HEp-2 cells. HEp-2 cells infected with the indicated strain were stained with polyclonal antisera against C227 (green) and counterstained with phalloidin-Alexa 568 (red) and DAPI (blue) to detect F-actin and nuclei, respectively. Scale bar=20 μm. (**b**) Relative expression of pAA genes that are differentially expressed *in vivo* (rabbit cecal fluid) vs *in vitro* (LB) at a false discovery rate < 0.01. Graphic and heat map representation of the 51 genes that are differentially expressed in two replicates of C227 *in vivo* relative to three replicates *in vitro*. The *Z* score reflects the degree of decreased (*Z* score < 0) or increased (*Z* score >0) abundance, computed by subtracting the mean of the log transformed expression values and dividing by the s.d. for each gene over all sampled scored. (**c**) Concentration (cfu g^{-1}) of bacteria recovered 2 or 3 days PI from intestinal

homogenates of tissues from rabbits infected with the indicated strain. Data points represent individual rabbits (55989, n=10; 55989ΔpAA, n=6). Bars show the geometric mean.

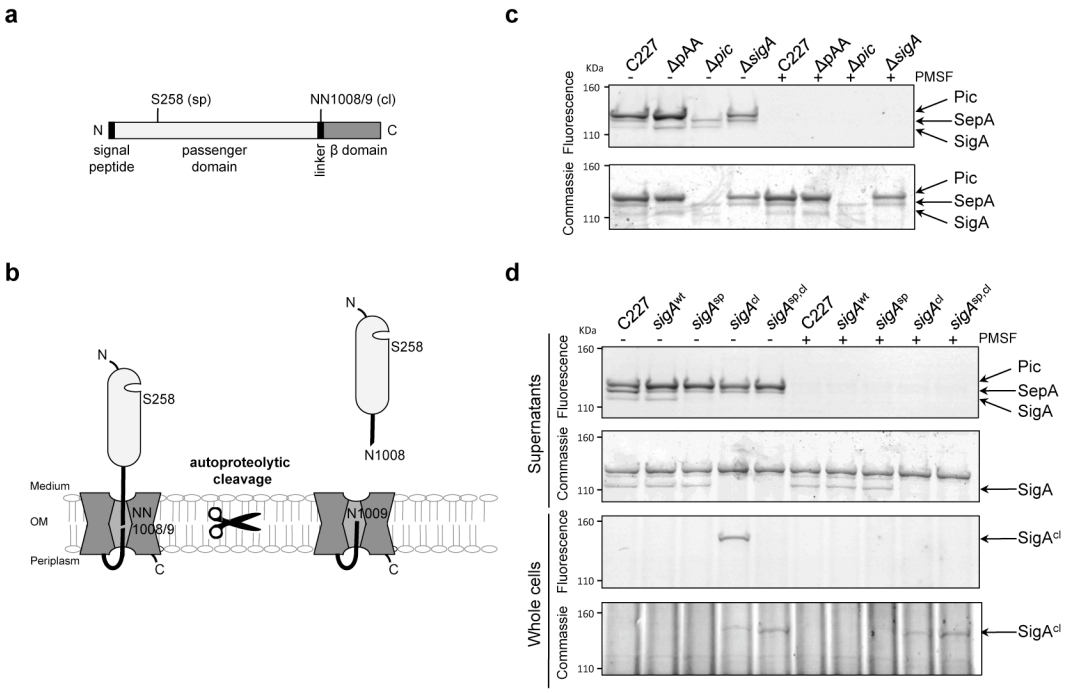

Figure 5. Activity of SPATEs from C227 and isogenic mutants

(**a**) Domain structure and predicted catalytic serine (sp) and autocleavage sites (cl) in SigA. (**b**) Schematic of SigA topology and processing. (**c**) Activity-based protein profiling of secreted SPATEs from C227. Supernatant from overnight cultures of the indicated strains were reacted with the serine hydrolase probe (TAMRA-FP), run on SDS-PAGE gels, and scanned to detect fluorescence or stained with commassie to visualize total protein. Control samples were incubated with PMSF, which specifically abolishes serine protease activity, prior to addition of TAMRA-FP. (**d**) Activity-based protein profiling of C227, its Δ*sigA* derivative complemented with *sigA*-wt, or the indicated *sigA* point mutants. Whole cells or supernatants from overnight cultures were assayed as in (**c**). Full fluorescence-scanned blots and coomassie-stained gels are shown in Supplementary Fig. 8.

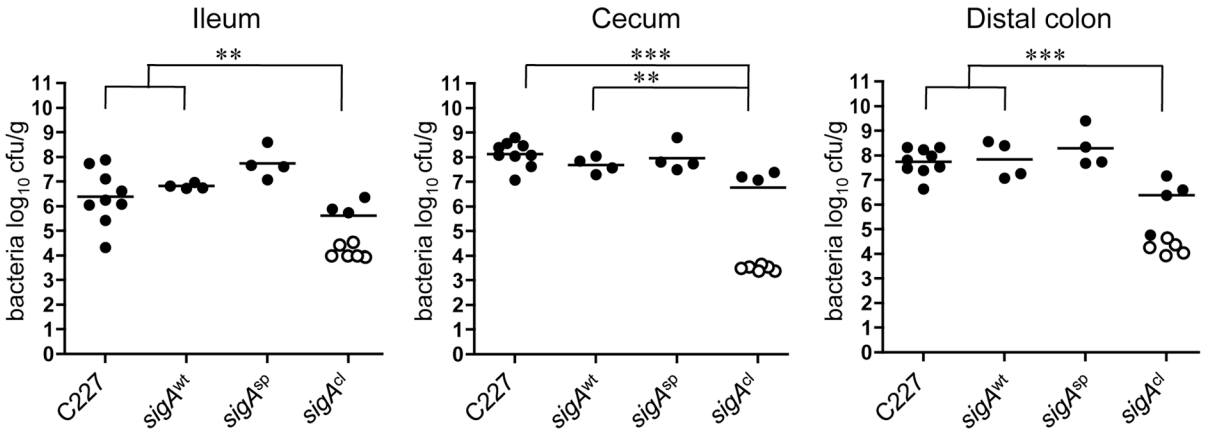

Figure 6. Intestinal colonization in infant rabbits inoculated with C227 or isogenic *sigA* point mutants

Concentration (cfu g^{-1}) of bacteria recovered 3 days PI from intestinal homogenates of tissues from rabbits infected with the indicated strain. Data points represent individual rabbits (C227, n=9; *sigA*^{wt}, n=4; *sigA*^{sp}, n=4; *sigA*^{cl}, n=9). Open symbols represent the limit of detection for samples from which no cfu were isolated. Bars show the geometric mean. Statistical analysis was performed using one way ANOVA and Bonferroni's multiple comparison post-test; ** $P < 0.01$ and *** $P < 0.001$.

Table 1

Diarrhea in infant rabbits inoculated with the indicated strains

Strain[a]	**C227**	**mock**	**Δ*stx2***	**ΔpAA**	**Δ*pic***	**Δ*sigA***
Diarrhea (%)[b]	73	0	0	71	36	15
Disease category (#)[c]						
Diarrhea	30	0	0	10	5	3
Intestinal fluid	9	0	2	3	7	10
No gross disease	2	9	13	1	2	7
Total no. animals	41	9	15	14	14	20
P-value vs C227[d]	-	6.704E-5	4.754E-7	1	0.0223	2.37E-5
P-value vs mock[d]	6.704E-5	-	1	1.60E-3	0.1157	0.5320

[a] All strains are derivatives of *E. coli* O104:H4 C227-11 wild type (C227).

[b] Percentage of rabbits that exhibited diarrhea by day 3 PI.

[c] Number of rabbits within each category as described in the methods.

[d] Fisher's exact test was used to compare the proportion of rabbits with diarrhea in the indicated group vs C227 or mock-infected animals.

Table 2

Diarrhea in infant rabbits inoculated with C227 or isogenic *sigA* point mutants

Strain[a]	**C227**	***sigA*^{wt}**	***sigA*^{sp}**	***sigA*^{cl}**
Diarrhea (%)[b]	73	67	71	17
Disease category (#)[c]				
Diarrhea	30	4	5	3
Intestinal fluid	9	2	1	8
No gross disease	2	0	1	7
Total no. animals	41	6	7	18
P-value vs C227[d]	-	1	1	1.18E-4

[a] All strains, except C227, are derivatives of C227⊗*sigA*, where the *sigA* deletion was replaced with *sigA*^{wt}, *sigA*^{sp} or *sigA*^{cl}. The C227 data is from Table 1.

[b] Percentage of rabbits that exhibited diarrhea by day 3 PI.

[c] Number of rabbits within each category as described in the methods.

[d] Fisher's exact test was used to compare the proportion of rabbits with diarrhea in indicated group vs C227.